

# Structural investigation of MnO-B<sub>2</sub>O<sub>3</sub>-PbO-Ag<sub>2</sub>O glass system by EPR spectroscopy

V. TIMAR, I. ARDELEAN\*

Faculty of Physics, Babes-Bolyai University, 400084, Cluj-Napoca, Romania

Glasses of the  $x\text{MnO}\cdot(100-x)[3\text{B}_2\text{O}_3\cdot(1-y)\text{PbO}\cdot y\text{Ag}_2\text{O}]$  systems, with  $0 \leq x \leq 20$  mol% and  $y = 0.1, 0.3, 0.5$  were prepared and investigated by means of electron paramagnetic resonance (EPR) measurements. The local order in diamagnetic vitreous matrices may be revealed by the  $\text{Mn}^{2+}$  paramagnetic ions used in EPR experiments. The concentration range in which homogeneous glasses systems are formed ( $0 \leq x \leq 20$  mol%) is not influenced on particular values of  $y$ . In each systems corresponding a particular value of  $y$ , the effect of increasing the MnO content in the samples was investigated. The EPR absorption spectra of all investigated samples exhibit two resonance signals that are characteristic for the  $\text{Mn}^{2+}$  ( $3d^5; {}^6S_{5/2}$ ) ions, centered at  $g_{\text{eff}} \cong 4.3$  and  $g_{\text{eff}} \cong 2.0$ . The relative intensity of these resonance lines depends on the MnO content in the samples, indicated the various distribution of the  $\text{Mn}^{2+}$  ions on different structural units of vitreous matrices. For  $x \leq 5$  mol%,  $g_{\text{eff}} \cong 2.0$  resonance line has a resolved hyperfine structure (hfs) characteristic for isolated  $\text{Mn}^{2+}$  ions. Hfs is superposed over the wide line, given by dipolar interactions between manganese ions. For  $5 < x \leq 20$  mol% concentration range, the resonance line from  $g_{\text{eff}} \cong 2.0$  not present hfs, indicating the structural modification in  $\text{Mn}^{2+}$  vicinity, gradually increasing of dipolar interactions and the appearance in small proportion of the super-exchange magnetic interactions ( $x > 1$  mol%). The resonance lines centered at  $g_{\text{eff}} \cong 4.3$  appear in the whole concentration range, have the small intensity, not present hfs and is attributed to isolated  $\text{Mn}^{2+}$  ions disposed in octahedral symmetric sites slightly tetragonally distorted. When increase the Ag<sub>2</sub>O content in glasses matrices, the shape of EPR spectra is little modified. In addition, it observed a similitude concerning the way of variation from the characteristic parameters of resonance lines (line intensity and line-width).

(Received November 1, 2008; accepted November 27, 2008)

**Keywords:** Silver-lead-borate glasses, Manganese ions, Local structure, EPR

## 1. Introduction

Valuable informations concerning the structural details of vitreous systems have been frequently obtained by means of the electron paramagnetic resonance (EPR) of  $\text{Mn}^{2+}$  ions used as paramagnetic probes. Many oxide glasses such as borate [1,2], silicate [3,4], phosphate [5], tellurite [6], bismuthate [7], chalcogenide [8,9] and halide [10,11] glasses doped with manganese ions were investigated. Thanks to great sensitivity of the EPR absorption spectra to symmetry and strength of the ligand field in the neighbourhood of paramagnetic ions, it obtained informations about the different structural units evolution, the strength of bonding, the valence state and the distribution mode of the manganese ions in the glass network.

Generally, the EPR absorption spectra of  $\text{Mn}^{2+}$  ( $3d^5; {}^6S_{5/2}; I=5/2$ ) ions in oxide glasses consist on resonance absorptions centered at  $g_{\text{eff}} \cong 4.3, 3.3$  and  $2.0$ , their relative intensity being strongly dependent on composition [4,10]. The  $g_{\text{eff}} \cong 4.3$  resonance line is typical of isolated  $\text{Mn}^{2+}$  ions disposed in cubic symmetric sites slightly tetragonally or rhombically distorted [6]. The  $g_{\text{eff}} \cong 3.3$  resonance absorption arises from isolated  $\text{Mn}^{2+}$  ions situated in octahedral vicinities subjected to strong crystalline field effects [4,5,11]. The  $g_{\text{eff}} \cong 2.0$  resonance absorption is assigned to isolated ions having signals with resolved hfs, as well as those implicated in dipolar [12] or/and super-exchange magnetic interactions [6].

The borate glasses are very often investigated because they are relatively easy to obtain, are relative stable glasses, representing good matrices for transitional metal ions and moreover because in their structure appears a large variety of structural units over a wide range of modifiers concentration [13,14]. Today, the borate glasses are known as important material for insulation (glass wool) and textile (continuous filament) fiberglass [15]. Lead borate oxide glasses are highly transparent in the visible and near-infrared regions and exhibit very good glass formation over a large compositional range [16]. The high ionic conductivity and numerous applications such as biomaterials with antibacterial and antimicrobial effects, biomaterials for cancer and HIV therapies, chemical sensors, electrochromic display devices and solid batteries [17-20] represent the mains points of interest on study of the glasses containing silver oxide.

This paper aims to present our results concerning the structural details of the  $3\text{B}_2\text{O}_3\cdot(1-y)\text{PbO}\cdot y\text{Ag}_2\text{O}$  vitreous matrices (with  $y = 0.1, 0.3$  and  $0.5$ ) gradually doped with MnO, revealing the  $\text{Mn}^{2+}$  ions distribution on various structural units also the interactions involving them. Investigations were made by EPR spectroscopy.

## 2. Experimental procedure

Three series of samples from  $x\text{MnO}\cdot(100-x)[3\text{B}_2\text{O}_3\cdot(1-y)\text{PbO}\cdot y\text{Ag}_2\text{O}]$  system, with  $y = 0.1, 0.3, 0.5$  were prepared using pure reagent grade compounds, i.e.

H<sub>3</sub>BO<sub>3</sub>, PbO, AgNO<sub>3</sub> and MnCO<sub>3</sub> in suitable proportions. The mixtures corresponding to the desired compositions were mechanically homogenized and melted in air, in sintered corundum crucibles, in an electric furnace at 950°C. For melting, the samples were put into the electric furnace directly at this temperature. The molten material was kept at this temperature for 15 minutes and then quenched at room temperature by pouring on the stainless-steel plates.

The structure of samples was analyzed by means of X-ray diffraction using a Bruker D8 ADVANCE X-ray Diffractometer with a graphite monochromator for CuK<sub>α</sub> radiation ( $\lambda = 1.54 \text{ \AA}$ ). The pattern obtained did not reveal any crystalline phase in the samples up to 20 mol% MnO.

EPR measurements were performed at room temperature using an ADANI Portable EPR PS 8400-type spectrometer, in the X frequency band (9.4 GHz) and a field modulation of 100 kHz. To avoid the alteration of the glass structure due to the ambient conditions, samples of equal quantities were enclosed immediately after preparation in the tubular holders of the same caliber.

### 3. Results and discussion

First of all, it remarked the fact that the concentration range in which homogeneous glasses from studied system are formed ( $0 \leq x \leq 20 \text{ mol\%}$ ) isn't influenced on particular values of  $y$ , which means that the crystallized agent status of Ag<sub>2</sub>O content wasn't evidenced in our system.

Recorded EPR spectra show resonance lines due to Mn<sup>2+</sup> ( $3d^5$ ;  ${}^6S_{5/2}$ ;  $I=5/2$ ) paramagnetic ions for all investigated concentrations. As can be observed in Fig. 1 (a, b and c), the shape of the EPR spectra strongly depends on the MnO content of the samples and is little influenced by the Ag<sub>2</sub>O concentration in matrices. The spectra consist mainly of resonance lines centered at  $g_{\text{eff}} \cong 2.0$  and  $g_{\text{eff}} \cong 4.3$  values, their relative intensity depending on the manganese content of the samples. The absorption line centered at  $g_{\text{eff}} \cong 2.0$  is prevalent in the spectra, depends on the Mn<sup>2+</sup> ions content in the samples and shows the hfs characteristic of the <sup>55</sup>Mn ( $I = 5/2$ ) isotope that is well resolved for glasses with  $x \leq 5 \text{ mol\%}$ . The hyperfine sextet is due to isolated Mn<sup>2+</sup> ions situated in high symmetric octahedral sites. The  $g$  factor and hyperfine coupling constant ( $A \cong 90 \text{ G}$ ) values and the well resolved hfs show the predominantly ionic character of the bonding between Mn<sup>2+</sup> and O<sup>2-</sup> ions generating the octahedral symmetric ligand field. Weak axial distortions are superimposed on this field, varying in intensity and orientation from the vicinity of manganese ions to another [21,22]. The hyperfine coupling constant,  $A$ , was approximated as separation between the lines of the central pair of the hfs sextet. At high manganese content ( $5 < x \leq 20 \text{ mol\%}$ ), the spectra reduces to a single absorption line, without hfs, centered at  $g_{\text{eff}} \cong 2.0$ , indicating the structural modification in Mn<sup>2+</sup> vicinity and increases of dipolar interactions, accompanied in small proportions of the super-exchange magnetic interactions. The hfs sextet superimposes on a large absorption line, the envelope of all contributions at this absorption having  $g_{\text{eff}} \cong 2.0$ .

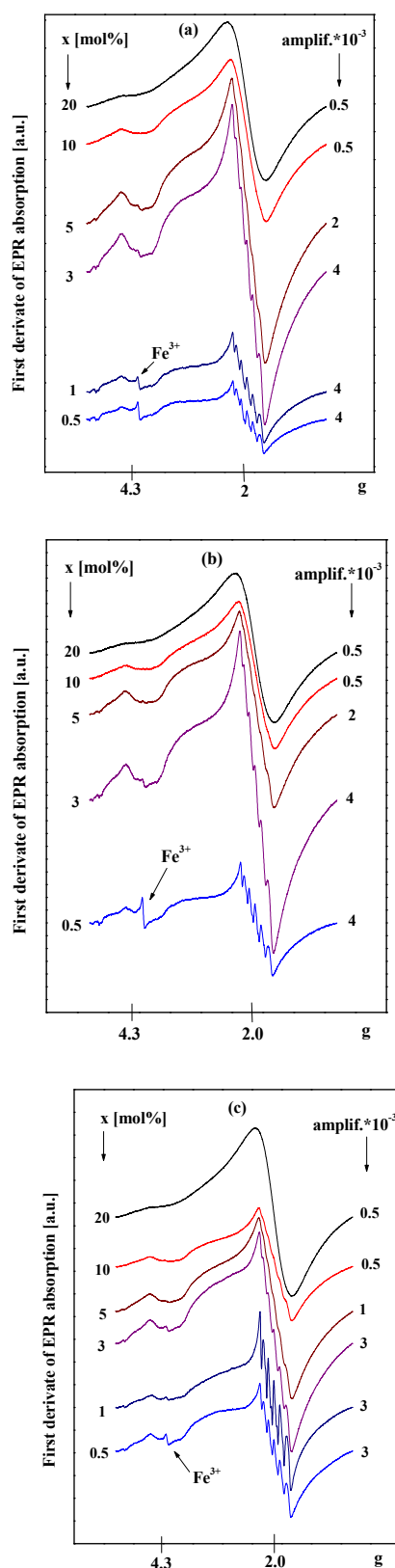


Fig. 1. EPR spectra of Mn<sup>2+</sup> ions in  $x\text{MnO} \cdot (100-x)[3\text{B}_2\text{O}_3 \cdot (1-y)\text{PbO} \cdot y\text{Ag}_2\text{O}]$  glasses with  $y = 0.1$  (a), 0.3 (b), 0.5 (c) and  $0.5 \leq x \leq 20 \text{ mol\%}$ .

The absorption line centered at  $g_{\text{eff}} \cong 4.3$  is less intense and doesn't show hfs (Fig.1). This resonance line, attributed to isolated  $\text{Mn}^{2+}$  ions disposed in cubic symmetric sites slightly tetragonally or rhombically distorted, appear in the whole concentration range and depends also on the  $\text{Mn}^{2+}$  ions content in the samples. Superimposed on this absorption line, the narrow line corresponding to accidental impurities of  $\text{Fe}^{3+}$  ( $3d^5$ ;  ${}^6S_{5/2}$ ) ions was also detected for  $x \leq 5$  mol% (Fig.1).

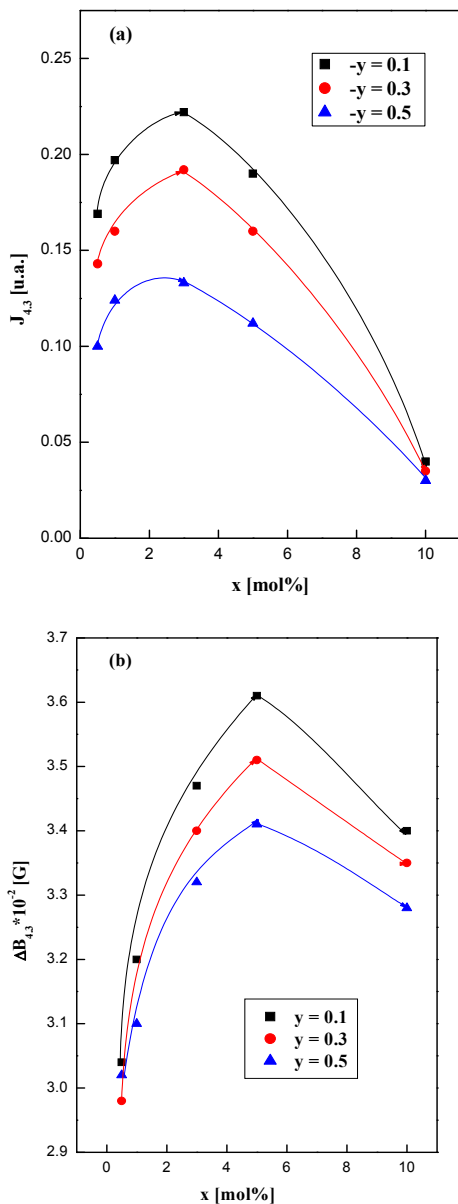


Fig. 2. Composition dependences of the line-intensity (a) and line-width (b) of resonance absorption at  $g_{\text{eff}} \cong 4.3$  for  $x\text{MnO} \cdot (100-x)[3\text{B}_2\text{O}_3 \cdot (1-y)\text{PbO} \cdot y\text{Ag}_2\text{O}]$  glasses, with  $y = 0.1, 0.3, 0.5$  and  $0.5 \leq x \leq 20$  mol%

The evolution of the resonance lines with increasing of manganese ions content was followed in the

dependence of the EPR characteristic parameters, i.e. the line intensity  $J$  (obtained as an integral of the area under the corresponding signal) and peak-to-peak line-width,  $\Delta B$ . The corresponding variations of these parameters are plotted in figures 2 and 3 for the resonance lines centered at  $g_{\text{eff}} \cong 4.3$  and respectively  $g_{\text{eff}} \cong 2.0$ . It remarked the fact that the analyzed parameters ( $J$  and  $\Delta B$ ) present the similar evolutions for these three series of investigated samples, but their effective values at the same  $x$  being smaller for great values of  $y$ . This result may be attributed to the decreasing of the  $\text{Mn}^{2+}$  ions concentration in the glasses structure following an increasing of the  $\text{Ag}_2\text{O}$  content in matrices. This fact releave the decisive status of vitreous matrix for distribution of  $\text{Mn}^{2+}$  ions in different structural sites that determine specific EPR absorption and nature/strength of interactions between them.

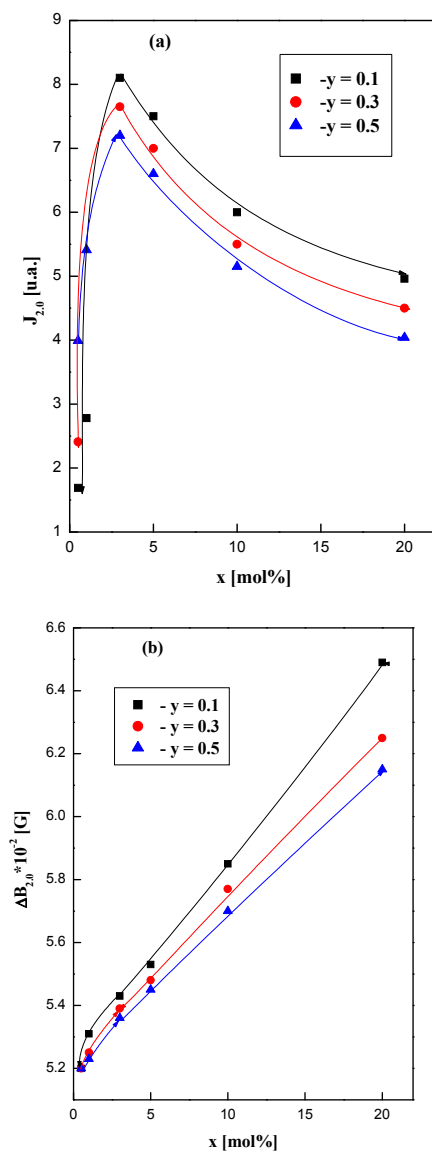


Fig. 3. Composition dependences of the line-intensity (a) and line-width (b) of resonance absorption at  $g_{\text{eff}} \cong 2.0$  for  $x\text{MnO} \cdot (100-x)[3\text{B}_2\text{O}_3 \cdot (1-y)\text{PbO} \cdot y\text{Ag}_2\text{O}]$  glasses, with  $y = 0.1, 0.3, 0.5$  and  $0.5 \leq x \leq 20$  mol%.

The  $g_{\text{eff}} \cong 4.3$  resonance line intensity has a complex evolution, showing an increasing in the concentration range  $0.5 \leq x \leq 3$  mol% followed by a decreasing for  $3 < x \leq 10$  mol% (Fig. 2(a)). For all the samples with composition corresponding to  $x = 20$  mol%, the resonance absorption at  $g_{\text{eff}} \cong 4.3$  is negligible. The structural units of defined symmetry involving Mn<sup>2+</sup> ions so that those to be isolated have at origin the structure of glass matrix former, B<sub>2</sub>O<sub>3</sub>. The concentration of Mn<sup>2+</sup> ions increase at the same time with the increasing of the MnO content in the samples. The decreasing of this resonance line intensity for higher concentration of MnO ( $x > 3$  mol%) is due to the modification of the configuration from the Mn<sup>2+</sup> ions neighbourhoods which no more assure their magnetic isolation. The line-width dependence of the  $g_{\text{eff}} \cong 4.3$  lines (Fig. 2(b)) shows an increasing up to  $x = 5$  mol% due to the increasing of Mn<sup>2+</sup> ions concentration [10,23]. This increasing is stopped in compositional range  $5 < x \leq 10$  mol%, due to the progressive decrease of the concentration of Mn<sup>2+</sup> ions disposed in structural configurations giving rise to the  $g_{\text{eff}} \cong 4.3$  absorptions.

The composition dependence of the  $g_{\text{eff}} \cong 2.0$  absorption line intensity is presented in figure 3(a). In the concentration range  $0.5 \leq x \leq 3$  mol%, the increasing of the MnO content in the samples determine an increasing of this line-intensity. Generally, the signal intensity is proportional to the number of EPR active species involved in the resonance absorption, so the increasing of the  $g_{\text{eff}} \cong 2.0$  line-intensity reflect an increase of the Mn<sup>2+</sup> ions concentration involved in other structural vicinities. Also, from analyse of the line-intensity variation with Ag<sub>2</sub>O content (Fig. 3(a)) result that in our glasses, at little concentration of MnO, increasing of the Ag<sub>2</sub>O content not favored rising of the Mn<sup>2+</sup> ions number which participate at the  $g_{\text{eff}} \cong 2.0$  resonance. Over  $x = 3$  mol%, the increasing of the MnO content in the samples determine an decreasing of line-intensity, due to the decreasing of Mn<sup>2+</sup> ions number and probably, appeared in studied glasses of the Mn<sup>3+</sup> ions, which do not manifest in EPR spectra at room temperature [24,25]. In vitreous oxide matrices, Mn<sup>3+</sup> ions have been frequently reported as progressively involved when increasing the MnO content [26-28]. The line-width of  $g_{\text{eff}} \cong 2.0$  lines depends also on the MnO concentration (Figure 3(b)), indicating an increase of this EPR characteristic parameter in whole concentration range. At  $x = 1$  mol% MnO appear a small decrease of slope in the curves what described the line-width evolution with the increasing of MnO concentration. This fact show that a little part of the Mn<sup>2+</sup> ions participate, beside dipolar, at the super-exchange interactions which determine relative narrowing of this resonance line. Also, increasing of the Ag<sub>2</sub>O concentration in the studied glasses determine decreasing of the effective values of the line-width. These data evidenced that the number of manganese ions which participate at super-exchange magnetic interactions increases with the increase of y.

#### 4. Conclusions

Homogeneous glasses of the three  $x\text{MnO} \cdot (100-x)[3\text{B}_2\text{O}_3 \cdot (1-y)\text{PbO} \cdot y\text{Ag}_2\text{O}]$  glass system, with  $y = 0.1, 0.3$  and  $0.5$  were obtained over the  $0 \leq x \leq 20$  mol% concentration range. EPR absorption spectra of these glasses has been analyzed to identify the manner of participations of Ag<sub>2</sub>O and MnO in the structure and to point out the role of the silver and manganese ions as a modifier of the glass network.

EPR absorption spectra due to Mn<sup>2+</sup> ions were recorded within  $0.5 \leq x \leq 20$  mol%. The shape of the spectra and the values of the EPR characteristic parameters of resonance lines depend on the MnO concentration. At the same time, the Ag<sub>2</sub>O content influenced the shape of EPR spectra, fact that is reflected by values of characteristic parameters of the resonance lines. This influence consists in decreasing of the J and  $\Delta B$  values at increasing of the y.

The isolated Mn<sup>2+</sup> ions disposed in cubic symmetric sites slightly tetragonally or rhombically distorted ( $g_{\text{eff}} \cong 4.3$ ) were detected over a broad concentration range, attesting the structural stability of the vitreous matrix in receiving these ions.

The line-width dependence of MnO content for resonance line centered at  $g_{\text{eff}} \cong 2.0$  indicate the structural modification in Mn<sup>2+</sup> vicinity and increases of dipolar interactions, accompanied in small proportions of the super-exchange magnetic interactions.

The vitreous structure of our glasses show an evolution with the MnO content from structural units involving Mn<sup>2+</sup> ions in well-defined vicinities having certain symmetry, to structural units containing clustered magnetic ions. The changes in shape of the  $g_{\text{eff}} \cong 4.3$  and  $g_{\text{eff}} \cong 2.0$  absorption lines when increasing the MnO content revealed this evolution.

#### References

- [1] D. L. Griscom, R.E. Griscom, *J. Chem. Phys.* **47**, 2711 (1967).
- [2] R. D. Dowsing, J.F. Gibson, *J. Chem. Phys.* **50**, 294 (1969).
- [3] H. H. Wickman, M.P. Klein, D.A. Shirley, *J. Chem. Phys.* **42**, 2113 (1965).
- [4] D. Loveridge, S. Parke, *Phys. Chem. Glasses* **12**, 19 (1971).
- [5] J. W. H. Schreurs, *J. Chem. Phys.* **69**, 2151 (1978).
- [6] I. Ardelean, M. Peteanu, G. Ilonca, *Phys. Stat. Solidi A* **58**, K33 (1980).
- [7] I. Ardelean, G. Ilonca, V. Simon, O. Cozar, V. Ioncu, S. Filip, *Solid State Commun.* **98**, 651 (1996).
- [8] R. C. Nicklin, C.P. Poole, H.A. Farach, *J. Chem. Phys.* **68**, 2579 (1973).
- [9] I. V. Chepeleva, E.A. Zhilinskaja, V.N. Lazukin, A.P. Cernov, V.I. Olkhovskii, *Phys. Stat. Solidi B* **82**, 189 (1977).

- [10] V. Cerny, B. Petrova, M. Frumar, J. Non-Cryst. Solids **125**, 17 (1990).
- [11] V. Cerny, B. Frumarova, J. Borsa, I.L. Licholit, M. Frumar, J. Non-Cryst. Solids **192-193**, 165 (1995).
- [12] O. Cozar, I. Ardelean, Gh. Ilonca, Solid State Commun. **44**, 809 (1982).
- [13] J. Wang, C.A. Angell, Glass Structure by Spectroscopy, Dekker, New York 1976, p.710.
- [14] E. I. Kamitsos, M.A. Karakassides, Phys. Chem. Glasses **30**, 19 (1989).
- [15] R. Akagi, N. Ohtori, N. Umesaki, J. Non-Cryst. Solids **293-295**, 471 (2001).
- [16] S. A. Nemilov, N.V. Romanova, Izv. AN SSSR. Neorg. Materialy **5**, 1247 (1969).
- [17] M. Dubiel, H. Hofmeister, G.L. Tan, K.D. Schicke, E. Wendler, Eur. Phys. J. D. **24**, 361 (2003).
- [18] J. L. Elechiguerra, J.L. Burt, J.R. Morones, Alejandra Camacho-Bragado, X. Gao, H.H. Lara, M.J. Yacaman, J. Nanobiotechnology **3**, 6 (2005).
- [19] S. Di Nunzio, M. Miola, E. Vernè, A. Massè, G. Maina, G. Fucale, Eur. Cells Mater. Vol. **10** Suppl. **1**, 22 (2005).
- [20] A. M. Mulligan, M. Wilson, J.C. Knowles, J. Biomed. Mater. Res. **A 2**, Vol. **67A**, 401 (2003).
- [21] M. Peteanu, I. Ardelean, S. Filip, D. Alexandru, Rom. J. Phys. **41**, 593 (1996).
- [22] I. Ardelean, S. Filip, J. Optoelectron. Adv. Mater. **5(1)**, 157 (2003).
- [23] D. L. Griscom, Glass Sci. Tech. **48**, 151 (1990).
- [24] D. L. Griscom, J. Non-Cryst. Solids **40**, 211 (1980).
- [25] E. Burzo, I. Ardelean, Phys. Stat. Solidi **B 87**, K173 (1978).
- [26] Gh. Ilonca, I. Ardelean, O. Cozar, J. Physique **49**, 8 (1988).
- [27] I. Ardelean, M. Peteanu, S. Filip, D. Alexandru, J. Magn. Magn. Mat. **157**, 239 (1996).
- [28] I. Ardelean, M. Peteanu, I. Todor, Phys. Chem. Glasses **43**, 276 (2002).

---

\*Corresponding author: arde@phys.ubbcluj.ro